ChemComm

Check for updates

Unravelling the spatial dependency of the complex solid-state chemistry of Pb in a paint micro-sample from Rembrandt's Homer using XRD-CT†

Stephen W. T. Price, [ID] *[ab] Annelies Van Loon,*[cde] Katrien Keune, [ID] *[ce]
Aaron D. Parsons, [ID] [b] Claire Murray, [ID] [b] Andrew M. Beale [ID] *[fg] and
J. Fred W. Mosselmans [ID] [b]

The surface of many Old Master paintings has been affected by the appearance of whitish lead-rich deposits, which are often difficult to fully characterise, thereby hindering conservation. A paint micro-sample from Rembrandt's Homer was imaged using X-ray Diffraction Computed Tomography (XRD-CT) in order to understand the evolving solid-state Pb chemistry from the painting surface and beneath. The surface crust was identified as a complex mixture of lead sulfates. From the S : Pb ratios throughout the paint layer, we can conclude that S is from an external source in the form of SO_2, and that the nature of Pb–SO_4 product is dependent on the degree of diffusion/absorption of SO_2 into the paint layers.

Several degradation phenomena disturbing the appearance of many Old Master paintings can be associated with the formation of lead soaps, of which the protrusions-small aggregates of lead soaps that 'protrude' through the paint surface- are the most researched.[1] Lead soaps or carboxylates are the consequence of reactions between lead pigments or driers and reactive carboxylic acid groups of the oil binder. This paper focuses on the formation of insoluble, whitish deposits on the surface of oil paintings (efflorescence), as yet another degradation phenomenon related to lead soaps. Complex crusts containing multiple inorganic phases have been identified using a number of state-of-the-art laboratory-based techniques.[1a,2] In all cases, the whitish surface crusts are insoluble salts rich in lead (Pb).

A clear understanding of the nature of the surface crust and underlying reaction processes is critical for guiding conservation strategies. We typically remove a tiny fragment of the painting after careful selection with a stereo-microscope, and prepare a paint cross-section for the investigation of the layer stratigraphy and composition of the paint. The use of synchrotron radiation (SR) X-ray microscopy techniques is essential for the study of these heterogeneous, multi-layered paint samples, offering the high spectral and spatial resolution that is required to characterize and localize the degradation products and their intermediate species present in low concentrations. SR X-ray fluorescence and X-ray absorption spectroscopy has proven a useful tool in identifying the form of Pb compounds, however cannot differentiate between very similar crystalline compounds, such as hydrocerrusite ($Pb_3(CO_3)_2(OH)_2$) and cerrusite ($PbCO_3$), or lead acetate ($Pb(C_2H_3O_2)_2$) and palmitate ($PbC_{32}H_{62}O_4$).[3]

Typical XRD measurements (with mm-sized beams) show lead white to be a mixture of cerussite and hydrocerussite, however the 2 micron resolution available at synchrotrons is able to spatially resolve the individual micro crystallites and their distributions within the paint layer. The use of SR microscopy has been successfully applied to characterise paint fragments by both FTIR and XRD 2-D mapping,[4] revealing chemical and phase distributions, and also by 3D X-ray tomography (absorption contrast),[5] providing information on voids and grain distribution within the paint layer. Mapping however, essentially interrogates the sample surface, thus is unable to provide the necessary depth information. In that regards, recently, a combination of XRD with computed tomography (XRD-CT[6]) has been demonstrated to be a powerful method for obtaining depth contrast and to identify with a spatial resolution in the μm, amongst other phases, plumbonacrite (3 $PbCO_3$· $Pb(OH)_2$·PbO) in a *ca.* 250 μm-wide, unembedded protrusion in *Wheat Stack Under a Cloudy Sky* (1889) by Vincent van Gogh.[7]

[a] Finden Ltd, Merchant House, 5 East St Helen Street, Abingdon, Oxfordshire, OX14 5EG, UK. E-mail: stephen@finden.co.uk

[b] Diamond Light Source, Harwell Science and Innovation Campus, Didcot, Oxon, OX11 0DE, UK

[c] Rijksmuseum, Ateliergebouw, Hobbemastraat 22, 1071 ZC, Amsterdam, The Netherlands. E-mail: K.keune@rijksmuseum.nl, A.van.loon@rijksmuseum.nl

[d] Royal Picture Gallery Mauritshuis, Plein, 29, 2511 CS, The Hague, The Netherlands

[e] Van't Hoff Institute for Molecular Science, University of Amsterdam, Science Park 904, 1098 XH, Amsterdam, The Netherlands

[f] Research Complex at Harwell, Rutherford Appleton Laboratory, Harwell Science and Innovation Campus, Didcot, Oxon, OX11 0FA, UK

[g] Department of Chemistry, University College London, 20 Gordon Street, London, WC1H 0AJ, UK. E-mail: Andrew.beale@ucl.ac.uk

† Electronic supplementary information (ESI) available: Reconstructed data is available at: 10.5281/zenodo.1237735. See DOI: 10.1039/c8cc09705d
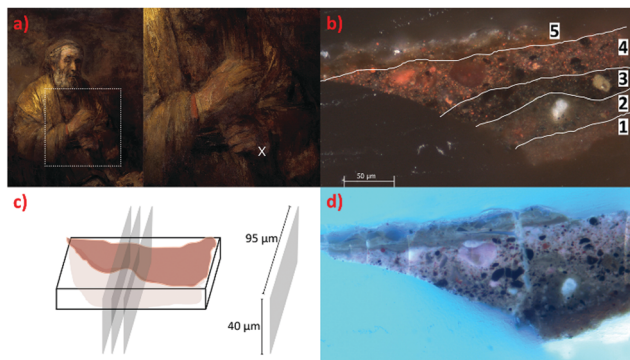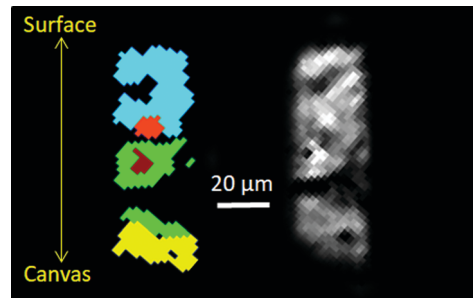
Fig. 1 Rembrandt van Rijn, Homer, 1663, oil on canvas, 107 × 82 cm, Mauritshuis, The Hague. Paint cross-section (X) taken from Homer's left hand (a), optical microscope showing layers of paint (b), schematic of paint fragment embedded in resin with dimensions and regions imaged (c), and UV (d).

Fig. 2 Cluster analysis (left) of XRD-CT (slice 1), and absorption-CT (Right), and diffraction patterns associated with each cluster are in the ESI† (Fig. S4). Each cluster corresponds to regions with similar diffraction patterns, and helps distinguish regions with different solid-state chemistry in the paint layer. Light blue is surface region, rich in lead sulfates, green is middle region, mainly lead soaps and lead white, yellow is bottom region by canvas, primarily calcite; the light and dark red regions correspond to two areas in the middle of the paint layer dominated by larger crystallites of lead white (hydrocerussite and cerussite).

In this study, μ-XRD-CT is used to address a fundamental question on the nature and formation of the whitish surface deposits rich in Pb, K and S-present in the form of sulfate as demonstrated by FTIR and Raman-found in Rembrandt's Homer (1663), Mauritshuis, The Hague. The deposits in this particular painting have been a topic of in-depth study since its last treatment in 2005/06.[2b,d,e] They cover most of the smalt and lake-rich, dark paint areas in this painting, Homer's garment, his cap, the background. For the μ-XRD-CT experiment (parameters see ESI†) a representative paint cross-section (Fig. 1) was selected that contained the complete layer structure. As such we note that this is for the first time that μ-XRD-CT was applied directly to a paint cross-section. In total three 2 μm-thick cross-sections of approximately 95 × 40 μm² of the embedded paint fragment were measured at 2 μm spatial resolution over a time of six hours. The known build up of the paint layers a priori (Fig. 1) helped confirm the orientation of the sample.

Each XRD-CT data set consists of thousands of XRD patterns. Whilst the data quality from a single pixel is sufficient to perform phase identification, the volume of data is prohibitive. Therefore cluster analysis (Fig. 2, also Fig. S4–S6, ESI†) was performed on the datasets, grouping together pixels with similar XRD pattern intensity and/or shape, such that the spatial information is preserved, whilst greatly reducing the number of XRD patterns, and can therefore be analysed in a reasonable timescale. This process also greatly improves the signal : noise ratio. Fitting of XRD-CT allows the identification of all Pb crystalline phases, even those present in minor amounts which are typically lost when trying to fit the summed XRD pattern (similar to bulk XRD). The complex variation in lead structures, and the deeper understanding of the chemistry occurring within the paint layer, can therefore only be identified by spatially resolved measurements such as XRD-CT. For all phases reported herein, the unique diffraction peaks (taken from the full pattern identification) used to identify the phase were present at the start and end of the measurement, indicating that none of these phases were formed by the X-ray beam. However, a reduction in intensity (ca. 15%) of some peaks for leadhillite and the lead

soaps was observed during the data collection, indicating that there was some beam interaction/damage.

The first orangey ground layer (1) (thickness ca. 15 μm) sits approximately between 80 and 95 μm beneath the surface of the paint and consists primarily of calcite ($CaCO_3$) and earth pigment. It corresponds to the yellow phase in Fig. 2. The distribution of calcite over the first slice is plotted in Fig. 3h (see also Fig. S7 and S8, ESI†). This is followed by a second ground layer (2) (ca. 20 μm) of mostly lead white that has converted into lead soaps. The loss of the original highly scattering particulate lead white pigment is significant, as can be seen by the less dense, amorphous character of the layer in the SEM-BSE images (Fig. S2, ESI†). The smallest crystallites are known to react first, leaving only a few large, highly scattering agglomerates remaining.[2d,e] Fitting of the XRD-CT identifies hydrocerussite (basic lead carbonate), as well as lead soaps (fitted as lead palmitate and lead azelate–$PbC_9H_{14}O_4$) in the second ground layer (Fig. 2, 3e, f and Fig. S4, S5, ESI†). The maps of hydrocerussite and cerussite do not overlap (Fig. 3f and g). Hydrocerussite is the main component of lead white.[8] Lead white can also contain a small fraction of cerussite (lead carbonate), usually varying between 5 and 10%, but it seems that most of the cerussite originally present in the second, lead white-containing ground layer has reacted away. The presence of lead soaps in the second, upper ground corroborates prior FTIR results (band at ca. 1520 cm⁻¹ characteristic of the lead carboxylate group $\nu_{as}COO$).[2b,e] The XRD patterns have a large background signal above 10 Å (in part due to the detector, but also due to the resin encapsulating the samples), and so reflections with large d-spacings are not well resolved. As such the largest intensity reflections (i.e. >6 Å) identified by Robinet and Corbeil[8a] cannot be used to assign the lead soaps present. However the pattern fitting matched well with structures reported by Catalano[9] and Plater.[10] A dark undermodelling paint (3) (bone black and earths; ca. 15 μm) was applied on top of the ground layers, followed by a reddish paint (4) (red earth, red lake, bone black, smalt; ca. 30 μm) and a smalt-containing glaze (5) (ca. 15 μm)
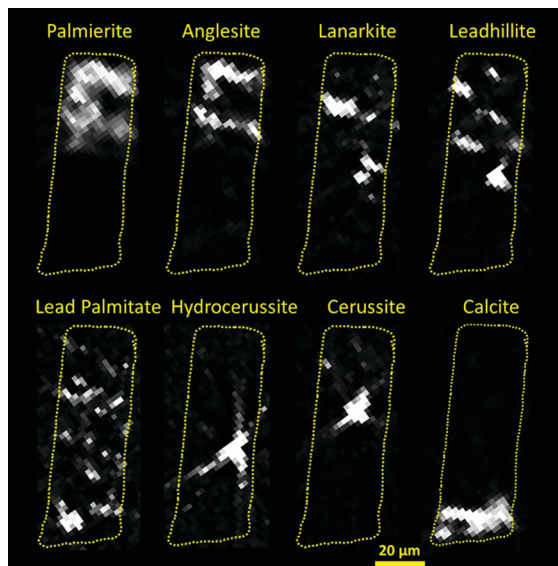
Fig. 3   Maps of the location of each major Pb containing phase for the Rembrandt fragment (slice 1). (a) palmierite, (b) anglesite, (c) lanarkite, (d) leadhillite, (e) lead palmitate, (f) hydrocerussite, (g) cerussite, (h) calcite. Dashed yellow outline over each phase marks the approximate boundaries of the sample as defined by the absorption reconstruction, and act as a guide to identify the relative location of each phase within the sample. Where possible the major reflection has been used to create the map of the phase (Table S2, ESI†), however this is not always possible, and so in certain cases a less intense reflection was used, this resulted in higher background noise (e.g. lanarkite). NB some streak artefacts are still present even after the application of the mean trimmed filter to the raw data (see ESI†), indicating the presence of large single crystals, e.g. hydrocerussite.

(Fig. 1 and Fig. S1, ESI†). The SEM-BSE images reveal many small lead-rich particles dispersed throughout these layers (3 to 5), as well as deposited at/near the paint surface (Fig. S2, ESI†).

Fitting of the XRD-CT reveals that these layers are rich in various lead sulfate and/or carbonate compounds; palmierite ($K_2Pb(SO_4)_2$), anglesite ($PbSO_4$), lanarkite ($Pb_2(SO_4)O$), leadhillite ($Pb_4SO_4(CO_3)_2(OH)_2$), and (hydro)cerussite, along with lead soaps (Table S1 (ESI†) and Fig. 2, cyan phase). Significantly, the S : Pb ratio decreases away from the surface of the painting. The spatial distribution of the sulfate phases suggests that in the surface layer, the more thermodynamically stable anglesite and palmierite are formed, which penetrate up to 30 μm beneath the surface (Fig. 3a and b). Moving beneath the surface layer, up to ca. 60 μm deep, the more rare lead minerals lanarkite and leadhillite are found (Fig. 3c and d). Some cerussite has formed deeper in the paint structure, approximately 30 to 40 μm beneath the paint surface (Fig. 3g).

The distribution of lead species throughout the sample as revealed by XRD-CT helps to build a theory about how insoluble lead-rich surface deposits may form. Fig. 4 shows a schematic diagram for the formation of the different Pb phases. Lead is solubilized from the lead white ground. It either reacts with free long-chain fatty acids (FA-C_{16} or FA-C_{18}) forming lead soaps, or becomes incorporated in the oil network binding to the carboxylic acid groups.[11] Recent research by the authors proposes that the released lead ions migrate upward via an ionic
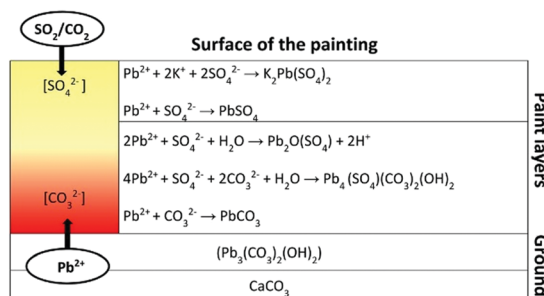

Fig. 4   Schematic diagram showing the formation and localisation of the different Pb phases in the painting.

driven mechanism ('ion hopping' over the carboxylic acid groups in the oil medium) into the upper layers.[12] There they form new mineral phases by interaction with atmospheric compounds. Sulfate formation is the preferential reaction in the upper paint layers. Leadhillite and lanarkite, as well as cerussite, were found deeper beneath the paint surface. The S : Pb ratio being greatest at the surface, suggests that external sources, most likely in the form of SO_2, are the origin of the sulfur. Combustion from domestic heating in the past may have released sulfurous gases into the atmosphere, as did the industrial revolution. The SO_2 is absorbed in or at the surface of the paint, where it readily oxidizes and reacts with moisture to form sulfates.[13] The presence of sulfur at/near the paint surface has previously been identified in other paintings.[2a,d,14] The Pb-phases also show the involvement of CO_3^{2-} ions in the formation of cerussite and leadhillite products. CO_2 from the atmosphere can form CO_3^{2-} ions, a comparable process as for SO_2. However, the CO_2 is not absorbed at the surface as much as SO_2, and therefore diffuses deeper into the paint structure.[15] We see comparable processes in large lead soap aggregates inside the painting, where lead soap is converted into lead carbonate and CO_2 is expected to play an important role.[2c] The availability of SO_4^{2-} and CO_3^{2-} ions and pH of the moisture in the paint system determine the lead phase formed. High SO_4^{2-} content and acidic environment favour anglesite formation over leadhillite and cerussite. This situation reflects the conditions at the paint surface, where anglesite and palmierite are the dominant Pb phases. Formation of leadhillite, lanarkite and cerussite require slightly different reaction conditions. Leadhillite is only stable at neutral environment, whereas cerussite is more likely to form at high CO_3^{2-} content and alkaline environment.[16c] The basic sulfate salt, lanarkite, is thermodynamically stable only at very low CO_3^{2-} content.[16a] Since historical paints are highly heterogeneous systems, the degree of alkalinity or acidity inside the system, as well as the amounts of SO_4^{2-} and CO_3^{2-}, can locally change and thereby influence the Pb phases formed. In turn, the chemical reactions that take place in the paint may also influence the local chemical environment, favouring the formation of other Pb phases. This can explain the variety of Pb phases including some rare minerals that co-exist deeper beneath the paint surface.

A remaining question is how has the palmierite formed from the Pb and K species. As earlier analysis of samples of Homer showed, the smalt used in the paint has almost completely discoloured due to the K leaching out to form water-soluble and

highly mobile K soaps.[2b–d] Previous research has shown that K soaps preferentially deposit at the paint surface.[2a] Although the smalt layer is relatively thin in this sample (5–10 μm), SEM-EDX mapping reveals a concentration of K at the surface away from the smalt particles (Fig. S2, ESI†). Exposure of K to SO_2 will also readily form water-soluble K sulfates. Pb ions seem to trap the K soaps/sulfates leading to the formation of insoluble crusts of palmierite. This process is probably similar to the formation of Pb-rich rims around organic lake pigment particles, the K_2SO_4-rich substrate adsorbing the migrated Pb and acting as direct reaction side for the formation of palmierite.[2b] The sulfates of Pb and Pb–K are highly insoluble in water or organic solvents, so it is not very likely that they migrate towards the surface once formed. This means that the anglesite and palmierite preferentially locate where they have formed, i.e. more towards the paint surface. Depending on how much K is available the ratio of anglesite to palmierite will change.

XRD-CT has been able to identify the different crystalline structures present, giving a clearer picture as to the nature of the Pb deposits, not just on the surface of the painting, but through the whole layer. The need for the mean trimmed filter applied to the data (see ESI†) strongly suggests that many of the crystallites identified are of dimensions equal to or larger than the beam size (2 μm), however the common presence of diffraction rings also indicates that much of the remineralisation that occurs results in many small (<1 μm) crystallites. The deeper understanding of the nature and likely pathway of formation of these sulfate and carbonate deposits has implications for the conservation treatment. The source of sulfur is historical, therefore, no new sulfurous deposits are expected to be formed if the crust will be removed. In this case study, however, a complete removal of those products would not be possible without damaging the original paint layer, since the surface deposits and the paint are so closely intertwined. In general, this case study demonstrates the complex Pb chemistry that takes place in mature oil paintings over time.

Conflicts of interest

There are no conflicts to declare.

Notes and references

1 (a) P. Noble and A. Van Loon, Art Matters Netherlands Technical Studies in Art, Zwolle, Waanders, 2007; (b) C. Higgitt, M. Spring and D. Saunders, National Gallery Technical Bulletin, London, 2003, vol. 24, pp. 75–95.

2 (a) M. Spring, C. L. Higgitt and D. R. Saunders, in Investigation of Pigment-Medium Interaction Processes in Oil Paint containing Degraded Smalt, London, 2005, vol. 26, pp. 56–70; (b) A. van Loon, Colour Changes and Chemical Reactivity in Seventeenth-Century Oil Paintings, PhD University of Amsterdam, Amsterdam, 2008; (c) K. Keune, A. van Loon and J. J. Boon, Microsc. Microanal., 2011, 17, 696–701; (d) A. van Loon, P. Noble and J. J. Boon, ICOM Committee for Conservation 16th Triennial Meeting, Lisbon, 2011; (e) A. van Loon, P. Noble and J. J. Boon in The formation of complex crusts in oil paints containing lead white and smalt: dissolution, depletion, diffusion, deposition, ed. N. Meeks, C. Cartwright, A. Meek and A. Mongiatti, Archetype, London, 2012, pp. 205–207.

3 (a) M. Cotte, E. Checroun, J. Susini and P. Walter, Appl. Phys. A: Mater. Sci. Process., 2007, 89, 841–848; (b) M. O. Figueiredo, T. P. Silva and J. P. Veiga, Appl. Phys. A: Mater. Sci. Process., 2006, 83, 209–211; (c) Y.-c. K. Chen-Wiegart, J. Catalano, G. J. Williams, A. Murphy, Y. Yao, N. Zumbulyadis, S. A. Centeno, C. Dybowski and J. Thieme, Sci. Rep., 2017, 7, 11656.

4 (a) M. Cotte, E. Checroun, V. Mazel, V. A. Solé, P. Richardin, Y. Taniguchi, P. Walter and J. Susini, e-Preserv. Sci., 2009, 6, 1–9; (b) N. Salvadó, S. Butí, M. J. Tobin, E. Pantos, A. J. N. W. Prag and T. Pradell, Anal. Chem., 2005, 77, 3444–3451.

5 E. S. B. Ferreira, J. J. Boon, J. van der Horst, N. C. Scherrer, F. Marone and M. Stampanoni, 3D synchrotron X-ray microtomography of paint samples, Proceedings of SPIE, O3A: Optics for Arts, Architecture, and Archaeology II, 2009, vol. 7391, p. 73910L, DOI: 10.1117/12.827511.

6 P. Bleuet, E. Welcomme, E. Dooryhée, J. Susini, J.-L. Hodeau and P. Walter, Nat. Mater., 2008, 7, 468.

7 F. Vanmeert, G. Van der Snickt and K. Janssens, Angew. Chem., 2015, 127, 3678–3681.

8 (a) L. Robinet and M.-C. Corbeil, Stud. Conserv., 2003, 48, 23–40; (b) V. Gonzalez, G. Wallez, T. Calligaro, M. Cotte, W. De Nolf, M. Eveno, E. Ravaud and M. Menu, Anal. Chem., 2017, 89, 13203–13211.

9 J. Catalano, A. Murphy, Y. Yao, G. P. A. Yap, N. Zumbulyadis, S. A. Centeno and C. Dybowski, Dalton Trans., 2015, 44, 2340–2347.

10 M. J. Plater, B. De Silva, T. Gelbrich, M. B. Hursthouse, C. L. Higgitt and D. R. Saunders, Polyhedron, 2003, 22, 3171–3179.

11 (a) J. J. Hermans, K. Keune, A. van Loon, R. W. Corkery and P. D. Iedema, RSC Adv., 2016, 6, 93363–93369; (b) J. van der Weerd, A. van Loon and J. J. Boon, Stud. Conserv., 2005, 50, 3–22.

12 (a) J. J. Hermans, K. Keune, A. van Loon and P. D. Iedema, J. Anal. At. Spectrom., 2015, 30, 1600–1608; (b) J. J. Hermans, K. Keune, A. van Loon and P. D. Iedema, Phys. Chem. Chem. Phys., 2016, 18, 10896–10905.

13 G. Thomson, Humidity, Butterworth-Heinemann, 1986, pp. 210–241.

14 (a) J. J. Boon and E. Oberthaler in Mechanical weakness and paint reactivity observed in the paint structure and surface of The Art of Painting by Vermeer, ed. S. Haag, E. Oberthaler and S. Penot, 2010, pp. 328–335; (b) M. Cotte, J. Susini, V. A. Sole, Y. Taniguchi, J. Chillida, E. Checroun and P. Walter, J. Anal. At. Spectrom., 2008, 23, 820–828.

15 (a) A. Czyżewski, J. Kapica, D. Moszyński, R. Pietrzak and J. Przepiórski, Chem. Eng. J., 2013, 226, 348–356; (b) F. A. Abdulsamad, J. H. Thomas, P. A. Williams and R. F. Symes, Mineral. Mag., 1982, 46, 499–501; (c) F. Abdul-Samad, J. H. Thomas, P. A. Williams, R. A. Bideaux and R. F. Symes, Transition Met. Chem., 1982, 7, 32–37; (d) N. H. Koralegedara, S. R. Al-Abed, S. K. Rodrigo, R. R. Karna, K. G. Scheckel and D. D. Dionysiou, Sci. Total Environ., 2017, 575, 1522–1529.